

RECENT RESULTS FROM NOvA

E. CATANO-MUR (for the NOvA Collaboration)

*Department of Physics, William & Mary,
Williamsburg, Virginia 23187, USA*

We present the most recent 3-flavor neutrino oscillation results from the NOvA long-baseline experiment, using a joint fit of $\nu_\mu \rightarrow \nu_\mu$, $\bar{\nu}_\mu \rightarrow \bar{\nu}_\mu$, $\nu_\mu \rightarrow \nu_e$, and $\bar{\nu}_\mu \rightarrow \bar{\nu}_e$ channels, and an accumulated exposure of 13.6×10^{20} protons-on-target of neutrino beam and 12.5×10^{20} protons-on-target of antineutrino beam. The best-fit values for the atmospheric parameters are $\Delta m_{32}^2 = (2.41 \pm 0.07) \times 10^{-3} \text{ eV}^2$, $\sin^2 \theta_{23} = 0.57_{-0.04}^{+0.03}$ and $\delta_{CP} = (0.82_{-0.87}^{+0.27})\pi$. The data disfavor combinations of oscillation parameters that lead to large asymmetries between the rates of ν_e vs $\bar{\nu}_e$ appearance.

1 Introduction

Neutrino oscillations are transitions in-flight between the flavor neutrinos, caused by non-zero neutrino masses and neutrino mixing. In the 3-flavor paradigm, the flavor eigenstates (ν_e, ν_μ, ν_τ) are linear combinations of three mass eigenstates (ν_1, ν_2, ν_3),

$$|\nu_\alpha\rangle = \sum_{i=1}^3 U_{\alpha i}^* |\nu_i\rangle, \quad \alpha = e, \mu, \tau, \quad (1)$$

where U is the unitary mixing matrix. The probabilities of flavor transitions will depend on: the elements of the mixing matrix, parameterized by three angles ($\theta_{12}, \theta_{13}, \theta_{23}$) and one phase (δ_{CP}); the squared differences between mass eigenvalues ($\Delta m_{21}^2, \Delta m_{32}^2$); the energy of the neutrino (E), and the distance it traveled (L).

Evidence of neutrino oscillations has been observed in solar, atmospheric, reactor and accelerator experiments. The different types of neutrino sources and experimental setups have characteristic values of L and E_ν , which set the ranges of $|\Delta m^2|$ and the kind of oscillations to which they are sensitive¹. In particular, long-baseline accelerator neutrino experiments have $L/E \sim 500 \text{ GeV/km}$, and are sensitive to the atmospheric-sector oscillations with a $\Delta m^2 \sim 2.5 \times 10^{-3} \text{ eV}^2$. With a primordially muon neutrino (or antineutrino) beam, the combined measurements of long-baseline disappearance ($\nu_\mu \rightarrow \nu_\mu$ and $\bar{\nu}_\mu \rightarrow \bar{\nu}_\mu$) and appearance ($\nu_\mu \rightarrow \nu_e$ and $\bar{\nu}_\mu \rightarrow \bar{\nu}_e$) allow the estimation of θ_{23} and Δm_{32}^2 , and the determination of the neutrino mass ordering ($\text{sign}(\Delta m_{32}^2)$), the octant of θ_{23} , and charge-parity (CP) violation in the neutrino sector.

2 The NOvA experiment

NOvA consists of two finely-segmented liquid-scintillator detectors operating 14.6 mrad off-axis from Fermilab's NuMI muon neutrino (or antineutrino) beam². The detectors comprise PVC cells filled with a liquid scintillator, arranged in planes that alternate between horizontal and

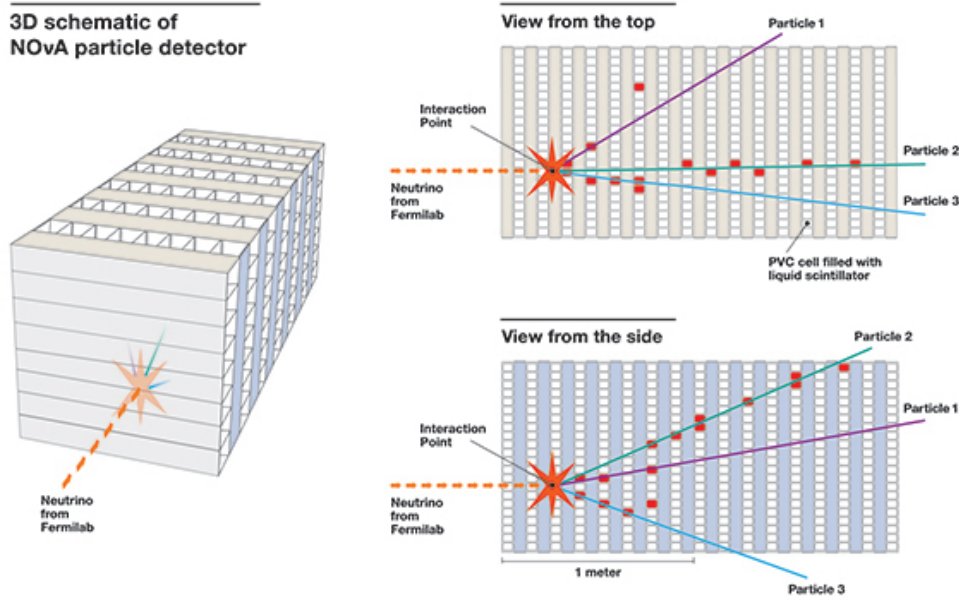


Figure 1 – Schematic of the NOvA detectors showing the alternating plane orientations. The combination of top and side views offers 3D reconstruction of the particle trajectory ⁵.

vertical directions to allow 3D reconstruction, as shown in Fig. 1. The near detector (ND) has 214 of such planes, and samples the beam 1 km from the source. The far detector (FD) has 896 planes, and observes the oscillated beam 810 km downstream, near Ash River, MN.

The data is collected in the detectors in the form of individual hits, which get clustered based on proximity in time and space to construct event candidates. These clusters are then processed to estimate the location of the interaction vertex, its direction, and other reconstructed quantities. Further, a convolutional neural network is used to classify the neutrino event candidates into ν_e CC, ν_μ CC, NC, or cosmogenic backgrounds. Figure 2 shows characteristic topologies of CC and NC events in the detectors.

The NOvA detectors are tracking calorimeters, and both characteristics are used to estimate the energy of the neutrino candidates. For ν_μ CC events, the energy of the muon is estimated using the track length ($\sim 4\%$ resolution), and the energy of the hadronic system is estimated using calorimetry ($\sim 30\%$ resolution). The ν_e CC energy is a function of the electromagnetic energy ($\sim 10\%$ resolution) and the hadronic energy, where both use calorimetry.

3 The NOvA oscillation analysis

Four channels are relevant to the estimation of neutrino oscillation parameters with NOvA: $\nu_\mu \rightarrow \nu_\mu$, $\bar{\nu}_\mu \rightarrow \bar{\nu}_\mu$, $\nu_\mu \rightarrow \nu_e$, and $\bar{\nu}_\mu \rightarrow \bar{\nu}_e$. The predictions of the spectra at the FD are constructed using a data-driven approach, using high-statistics measurements with the ND to improve the base simulation and constrain systematic uncertainties. For both appearance and disappearance, the signal predictions are corrected using ν_μ CC ND samples, for neutrino or antineutrino beam mode separately. The ν_e CC ND samples are used to correct the background predictions for the appearance channel.

NOvA's latest measurements of neutrino oscillation parameters ³ use data recorded between 2014 and 2020 and correspond to 13.6×10^{20} protons-on-target of neutrino beam and 12.5×10^{20} protons-on-target of antineutrino beam. Figures 3 and 4 show the energy spectra of the ν_μ CC, $\bar{\nu}_\mu$ CC, ν_e CC and $\bar{\nu}_e$ CC candidates observed in the FD, compared to the best fit predictions. Table 1 summarizes the event counts for each sample, comparing the observations with the estimated signal, background and total predictions.

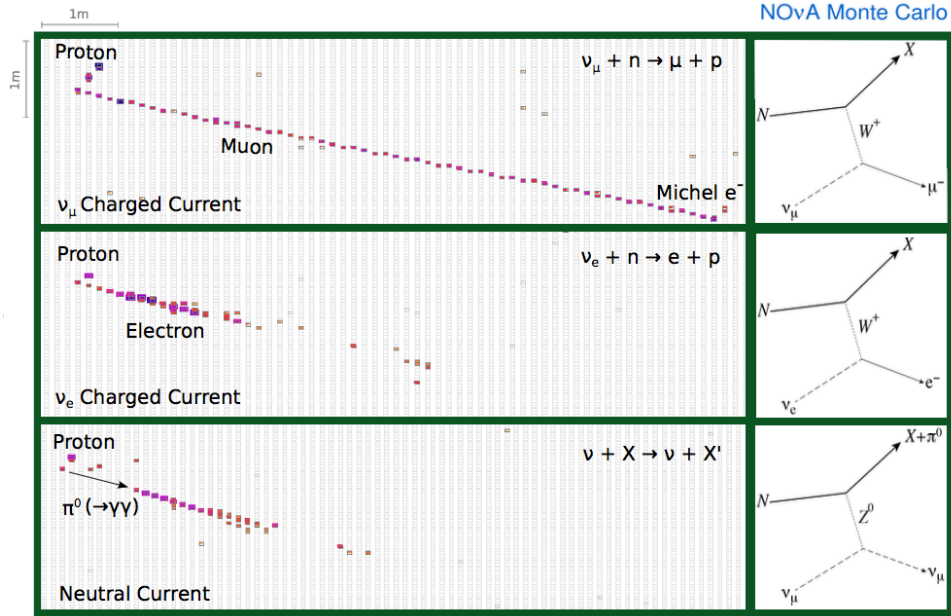


Figure 2 – Simulated neutrino interactions in the NOvA detectors: ν_μ CC (top), ν_e CC (middle), and NC (bottom)⁴.

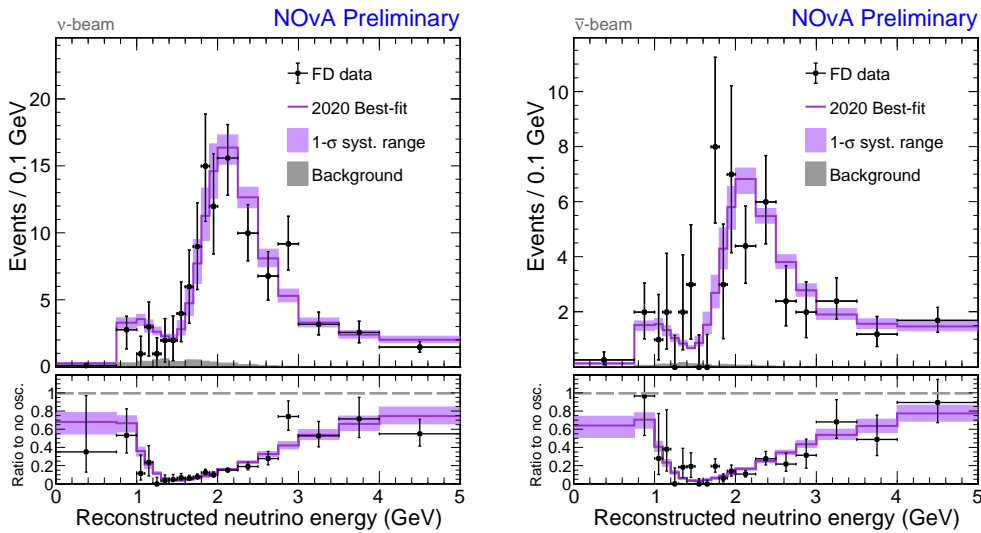


Figure 3 – Reconstructed neutrino energy spectra for the ν_μ CC (left) and $\bar{\nu}_\mu$ CC (right) samples at the FD.

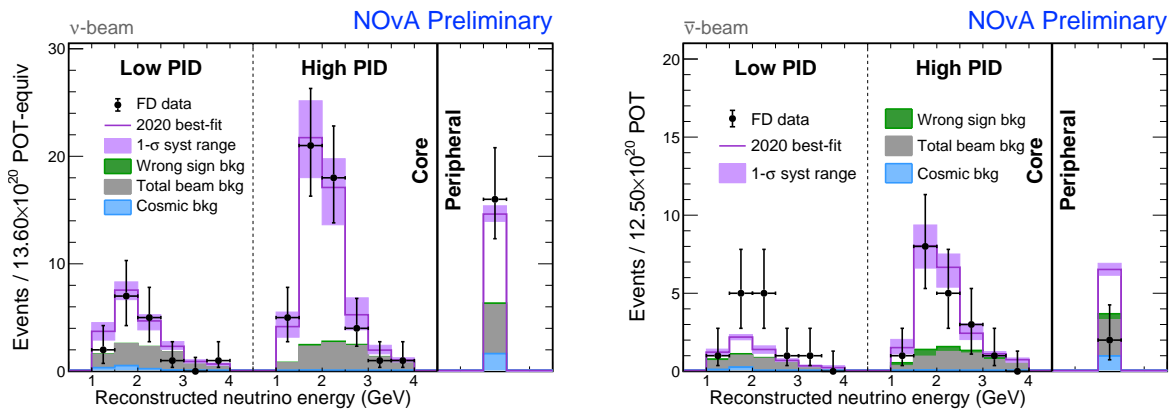


Figure 4 – Reconstructed neutrino energy spectra for the ν_e CC (left) and $\bar{\nu}_e$ CC (right) samples at the FD.

Table 1: Event counts at the FD, both observed and predicted at the best-fit point (Eq. 2).

	Neutrino beam		Antineutrino beam	
	ν_μ CC	ν_e CC	$\bar{\nu}_\mu$ CC	$\bar{\nu}_e$ CC
Signal	$214.1^{+14.4}_{-14.0}$	$59.0^{+2.5}_{-2.5}$	$103.4^{+7.1}_{-7.0}$	$19.2^{+0.6}_{-0.7}$
Background	$8.2^{+1.9}_{-1.7}$	$26.8^{+1.6}_{-1.7}$	$2.1^{+0.7}_{-0.7}$	$14.0^{+0.9}_{-1.0}$
Best fit	222.3	85.8	105.4	33.2
Observed	211	82	105	33

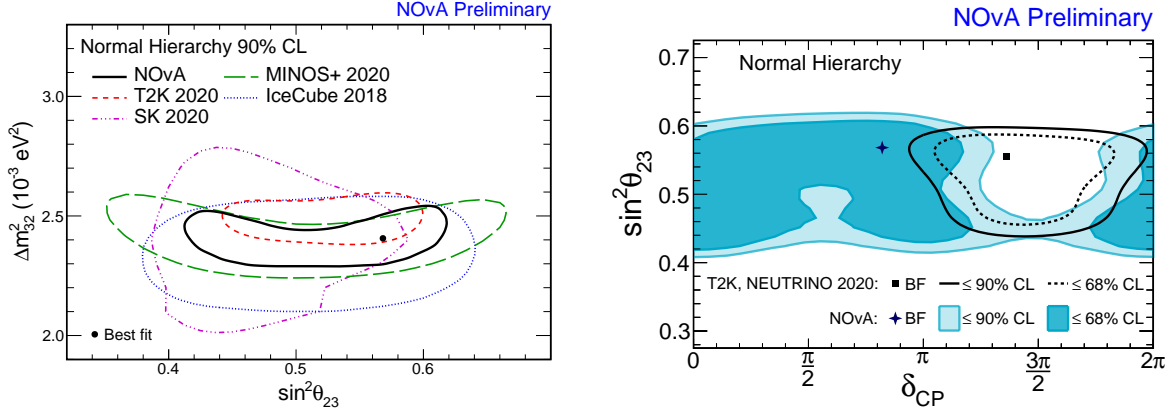


Figure 5 – Left: The 90% confidence level region for Δm_{32}^2 and $\sin^2 \theta_{23}$, comparing the NOvA allowed region (black) with the contours from other experiments^{6,7,8,9}. Right: The 68% and 90% confidence level regions for $\sin^2 \theta_{23}$ vs. δ_{CP} in the normal mass ordering, comparing the NOvA allowed regions (color areas) with the T2K contours⁶.

The best-fit parameters are obtained by minimizing a Poisson negative log-likelihood ratio between oscillated FD predictions and the observed spectra³. The fit includes three parameters that are allowed to vary freely ($\Delta m_{32}^2, \sin^2 \theta_{23}, \delta_{CP}$); 67 systematic uncertainties; and constraints from solar and reactor experiments ($\Delta m_{21}^2 = 7.53 \times 10^{-5} \text{ eV}^2$, $\sin^2 \theta_{12} = 0.307$, and $\sin^2 \theta_{13} = 0.0210 \pm 0.0011$). The resulting best-fit oscillation parameters (and their 1σ allowed ranges) are:

$$\begin{aligned} \Delta m_{32}^2 &= (+2.41 \pm 0.07) \times 10^{-3} \text{ eV}^2, \\ \sin^2 \theta_{23} &= 0.57^{+0.03}_{-0.04}, \\ \delta_{CP} &= (0.82^{+0.27}_{-0.87})\pi. \end{aligned} \quad (2)$$

The data disfavor combinations of parameters that lead to a strong asymmetry in the rate of ν_e vs $\bar{\nu}_e$ appearance: $\delta_{CP} = \pi/2$ is excluded at more than 3σ in the inverted mass ordering, and $\delta_{CP} = 3\pi/2$ in the normal ordering is disfavored at 2σ confidence. Considering all permutations of the mass ordering and the octant, degeneracies are such that all values of δ_{CP} are compatible with the data, with no preference of CP conservation over CP violation³.

Figure 5 shows 2-dimensional allowed regions for NOvA compared to other experiments, for the normal mass ordering. The $\Delta m_{32}^2 \times \sin^2 \theta_{23}$ contours show consistency among atmospheric and accelerator neutrino oscillation experiments. In the $\sin^2 \theta_{23} \times \delta_{CP}$ contours, the best-fit point of the T2K experiment lies in a region disfavored by this analysis, but regions of overlap remain³. This purported tension is not observed in the inverted mass ordering. The T2K and NOvA collaborations are working towards a joint neutrino oscillation analysis using both experiments' data sets simultaneously¹⁰.

NOvA is expected to take data through 2026, and the current projection for the ultimate exposure is $60\text{-}70 \times 10^{20}$ protons-on-target, approximately doubling the data analyzed so far¹¹. Figure 6 shows some projections for the resolution of the neutrino mass ordering and CP vio-

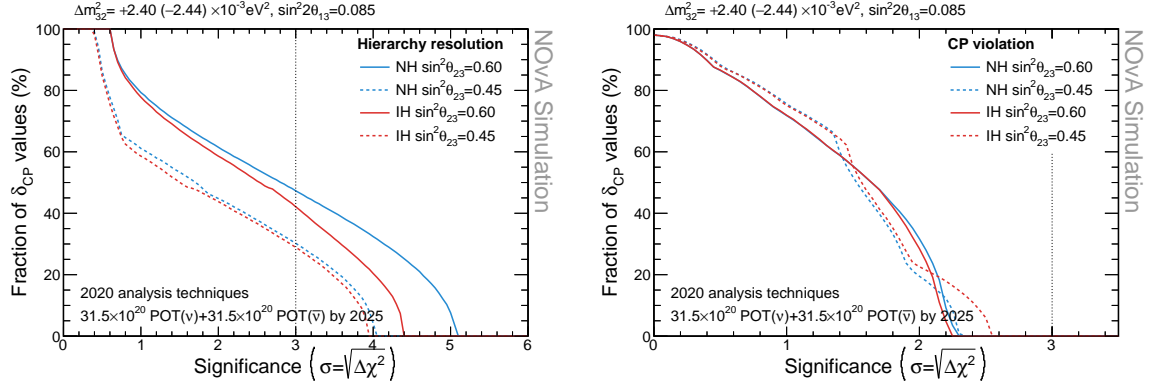


Figure 6 – Fraction of δ_{CP} values in the range $[0, 2\pi]$ for which the neutrino mass ordering (left) or CP non-conservation (right) could be resolved by NOvA at a given sensitivity σ by the year 2025, assuming an accumulated exposure of 63×10^{20} protons-on-target. The lines correspond to different true values of $\sin^2 \theta_{23}$ and true normal ordering (blue) or inverted ordering (red).

lation. NOvA could reach 2σ determination of CP violation, 3σ sensitivity to the ordering for 30-50% of δ_{CP} values, and up to $\sim 5\sigma$ in the most favorable case.

Acknowledgments

This document was prepared by the NOvA collaboration using the resources of the Fermi National Accelerator Laboratory (Fermilab), a U.S. Department of Energy, Office of Science, HEP User Facility. Fermilab is managed by Fermi Research Alliance, LLC (FRA), acting under Contract No. DE-AC02-07CH11359. This work was supported by the U.S. Department of Energy; the U.S. National Science Foundation; the Department of Science and Technology, India; the European Research Council; the MSMT CR, GA UK, Czech Republic; the RAS, RFBR, RMES, RSF, and BASIS Foundation, Russia; CNPq and FAPEG, Brazil; STFC, UKRI, and the Royal Society, United Kingdom; and the State and University of Minnesota. We are grateful for the contributions of the staffs of the University of Minnesota at the Ash River Laboratory and of Fermilab.

References

1. P.A. Zyla *et al.* [Particle Data Group], PTEP **2020**, no.8, 083C01 (2020) and 2021 update doi:10.1093/ptep/ptaa104
2. P. Adamson *et al.*, Nucl. Instrum. Meth. A **806**, 279-306 (2016).
3. M. A. Acero *et al.* [NOvA Collaboration], [arXiv:2108.08219 [hep-ex]].
4. M. Baird, J. Bian, M. Messier, E. Niner, D. Rocco and K. Sachdev, J. Phys. Conf. Ser. **664**, no.7, 072035 (2015)
5. Fermilab Creative Services, <https://vms.fnal.gov/>.
6. K. Abe *et al.* [T2K], Phys. Rev. D **103**, no.11, 112008 (2021).
7. Y. Nakajima [Super-Kamiokande], Neutrino 2020 conference, <https://doi.org/10.5281/zenodo.4134680>
8. P. Adamson *et al.* [MINOS+], Phys. Rev. Lett. **125**, no.13, 131802 (2020).
9. M. G. Aartsen *et al.* [IceCube], Phys. Rev. Lett. **120**, no.7, 071801 (2018).
10. R. Patterson *et al.*, Snowmass 2021 LOI https://www.snowmass21.org/docs/files/summaries/NF/SNOWMASS21-NF1_NFO_Ryan_Patterson-093.pdf
11. P. N. Shanahan *et al.* [NOvA], Eur. Phys. J. ST **230**, no.24, 4259-4273 (2021) doi:10.1140/epjs/s11734-021-00285-9